Nonlinear active noise control for a system with a nonminimum-phase secondary path

Liping Zhu (1), Jie Pan (2), Tiejun Yang (1) and Xuhao Du (2)

(1) College of Power and Energy Engineering, Harbin Engineering University, 145 Nantong Street, Harbin, Heilongjiang 150001, China
(2) School of Mechanical and Chemical Engineering, The University of Western Australia, 35 Stirling Highway, Crawley, WA 6009, Australia

ABSTRACT

In this paper, a nonminimum-phase secondary path measured inside a car is analysed and its influence on noise reduction is discussed. To improve control performance, a new nonlinear algorithm using a configuration with a bilinear filter and trigonometric expansions is proposed for a control system with a nonminimum-phase secondary path. Within the controller of an adaptive feedforward control system, the proposed algorithm achieves high-order nonlinearities and has a better ability to predict a non-Gaussian signal. The application of this algorithm in reducing the interior road noise of a car is illustrated through simulations. Since road noise is complicated, six acceleration signals from a car's body are adopted as reference signals and one loudspeaker is used as an actuator to reduce noise near one microphone. The simulation results show that the proposed algorithm achieves better results than a traditional linear algorithm.

1 INTRODUCTION

Active noise control (ANC) techniques have been widely used for cancelling low-frequency noise and most ANC systems adopt a filtered-x least mean square (FXLMS) algorithm for its simplicity (Widrow, 1990; Kuo and Morgan, 1995). Unfortunately, the performance of the FXLMS algorithm relies heavily on the secondary path characteristics. To improve control results, we must increase the modelling accuracy of the secondary path by using effective offline and even online modelling algorithms (Hansen *et al*., 2012; Akhtar *et al*., 2006; Yang *et al*., 2018). However, if the secondary path is a nonminimum-phase system, then even perfect modelling cannot lead to a satisfactory result (Strauch and Mulgrew, 1998).

A nonminimum-phase secondary path has at least one zero on the right side of complex plane for a continuous system or at least one zero outside the unit circle for a discrete system (Oppenheim *et al*., 1996). It is usually caused by low-pass filtering of a controller, a time delay between actuators and sensors, and so on. A nonminimum-phase characteristic has a significance influence on the control system and is the main limitation for improving the control performance of both the FXLMS algorithm (Milani *et al*., 2010) and the robust control algorithm (Loiseau *et al*., 2015). In this paper, we will analyse the influence of the nonminimum phase for designing a controller and propose a new control algorithm to improve control performance for a control system with a nonminimum-phase secondary path.

The organisation of this paper is as follows. In Section 2, a nonminimum-phase secondary path measured in a car is analysed and its impact on controller design is discussed. A new nonlinear controller and control structure is proposed theoretically in Section 3. In Section 4, some simulations are conducted and conclusions are presented in Section 5.

2 ANALYSIS OF A NONMINIMUM-PHASE SECONDARY PATH

A secondary path is the signal transmission path from the output of a controller to the input of the controller. It includes a D/A converter, actuators, sensors, low-pass filter, and an A/D converter. We need to identify the secondary path before noise control is applied. In our experiment, the frequency band of interest is below 200 Hz. Therefore, we identified a secondary path with a bandlimited noise of 0–230 Hz using a least mean square method (Kuo and Morgan, 1995). The sampling frequency is 1600 Hz.

The frequency response of the identified secondary path is shown in Figure 1(a). It can be seen that the working range of the secondary path is 20–210 Hz and that out of that range the response is very low and the actuator has

no ability to reduce the corresponding frequency components. The zeros and poles distribution of the secondary path is shown in Figure 1(b). Since we only care about the frequency range 0–230 Hz, which is located in the sector indicated by the double-headed arrow in Figure 1(b), we can ignore the other zeros and poles outside of this frequency band. The reason zeros outside of the frequency band of interest are located almost on the unit circle is because we did not model that frequency range and the response of the secondary path is very low, which is equal to all zeros located on the unit circle. It can be seen that the secondary path has three pairs of conjugate zeros outside the unit circle in the frequency range of interest. Therefore, it is a nonminimum-phase system.

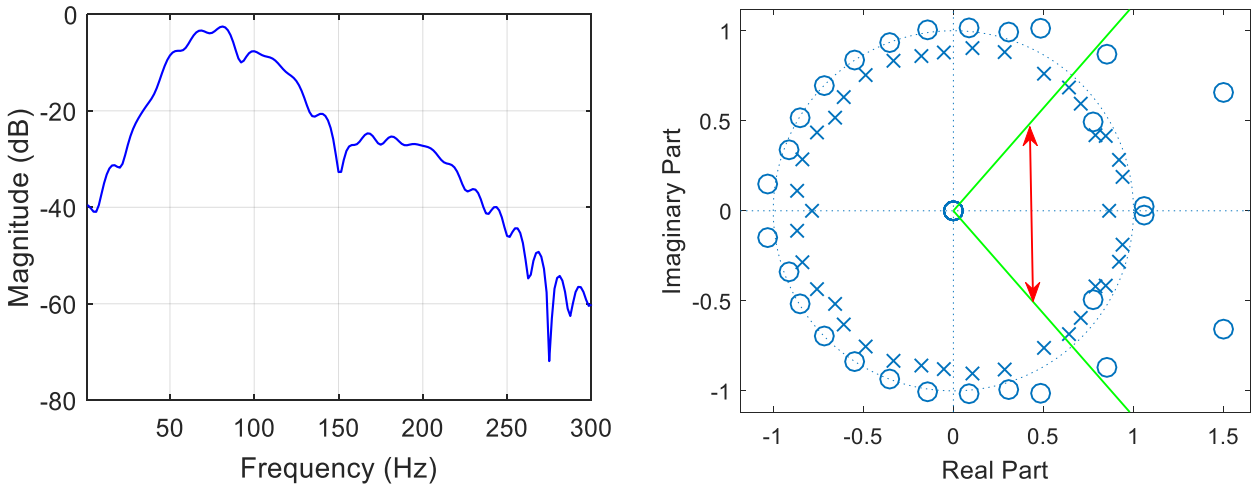

(a) (b)

Figure 1: Characteristics of the secondary path: (a) frequency response and (b) distribution of zeros (crosses) and poles (circles).

A block diagram of a control system based on the FXLMS algorithm is shown in Figure 2(a) (Strauch and Mulgrew 1998), where $P(z)$ and $S(z)$ are the primary and secondary paths, $W(z)$ is the controller, $d(n)$ and $\hat{d}(n)$ are undesired signal and output signal of an actuator. The ideal controller has the following expression:

$$W(z) = \frac{P(z)}{S(z)}. \tag{1}$$

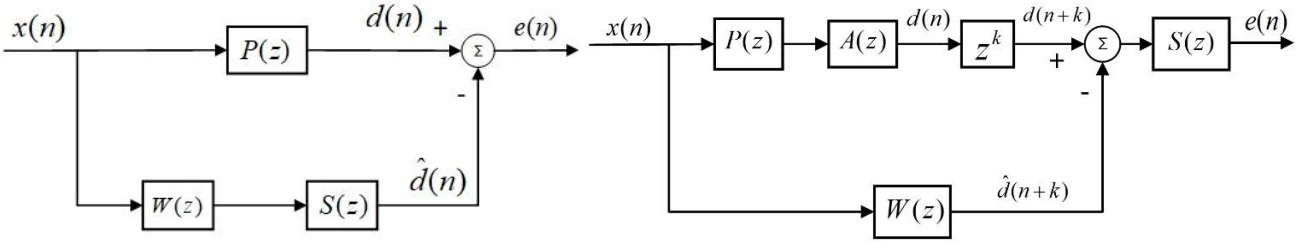

(a) (b)

Figure 2: The principles of the ANC system: (a) block diagram of the FXLMS algorithm and (b) the equivalent form of the FXLMS algorithm with a nonminimum-phase secondary path.

If the secondary path $S(z)$ is a nonminimum-phase system, then the secondary path $S(z)$ and its causal approximated inverse $A(z)$ satisfy following formulation (Widrow 1990):

$$S(z)A(z) = z^{-k}. \tag{2}$$

Thus, the optimal controller has the expression $W(z) = z^k A(z)P(z)$ and its equivalent control diagram is as shown in Figure 2(b). It is assumed that $H(z) = P(z)A(z)$ and the impulse response of $H(z)$ is $h_i,\ i = 0, \cdots, N-1$. According to Figure 2(b), the undesired signal is:

$$d(n+k) = \sum_{i=0}^{N-1} h_i x(n+k-i) = \sum_{i=0}^{k-1} h_i x(n+k-i) + \sum_{i=k}^{N-1} h_i x(n+k-i)\,. \tag{3}$$

The first part of the above equation is a linear combination of the future input signal with the system impulse response and the second part is a linear combination of the current and past inputs with the system impulse response. For the controller $W(z)$, its output signal $\hat{d}(n+k)$ is based on the past input signal $\boldsymbol{x}_{ref}(n)$ and can be expressed as:

$$\hat{d}(n+k) = E[d(n+k) \mid \boldsymbol{x}_{ref}(n)]\,. \tag{4}$$

Thus, the controller $W(z)$ is a predictor to predict the future undesired signal $d(n+k)$ based on the past input signal $\boldsymbol{x}_{ref}(n)$. From Eq. (3), we know that the second part of the undesired signal can be predicted by a linear control filter using the past input signal. Meanwhile, to predict the first part, it needs the future input, which is impossible for the controller to obtain. If the input signal $x(n)$ is a sinusoidal signal, then it is easy to predict the two parts of the undesired noise with a linear filter. However, if the input signal is non-Gaussian and is not independent from sample to sample, then, based on Eq. (3), we know that a linear filter can only predict the second part of the undesired noise and the first part cannot be predicted. Under this situation, a nonlinear filter will be required.

3 CONTROLLER DESIGN

In this part, we design a nonlinear controller to reduce the interior noise of a car. The structure of the controller is shown in Figure 3, where $f(\bullet)$ is defined as $f(x(n)) = \{x(n), \sin(\pi x(n)), \cos(\pi x(n))\}$ to yield high-order nonlinearities, and $S(z)$ and $\hat{S}(z)$ denote respectively the secondary path and the identified secondary path filter. The adaptive filter $W(z)$ has a bilinear filter structure and the input–output cross terms are added into the reference signal, so that the proposed bilinear filtered trigonometric expansions least mean square (BFTLMS) algorithm can achieve a satisfactory result with a short memory length.

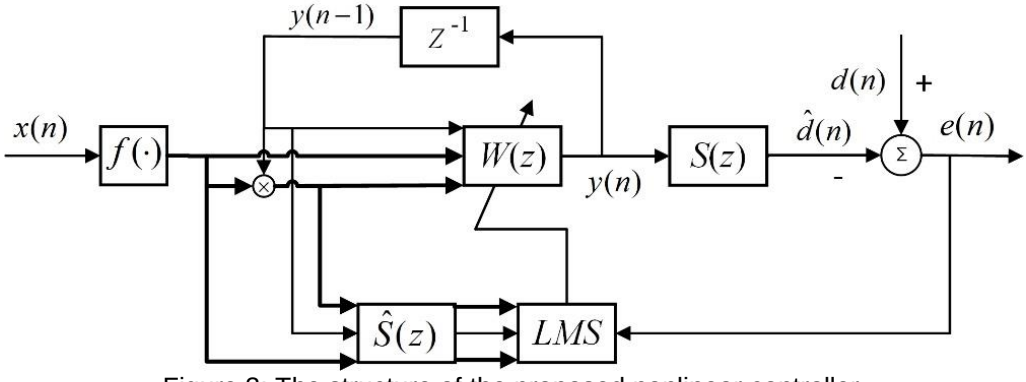

Figure 3: The structure of the proposed nonlinear controller.

Based on Figure 3, the output of the adaptive filter is:

$$y(n) = \boldsymbol{x}^T(n)\boldsymbol{w} = \boldsymbol{x}_1^T(n)\boldsymbol{w}_1 + \boldsymbol{x}_s^T(n)\boldsymbol{w}_s + \boldsymbol{x}_c^T(n)\boldsymbol{w}_c + \boldsymbol{y}^T(n-1)\boldsymbol{w}_y + \boldsymbol{c}^T(n)\boldsymbol{w}_{cross} \tag{5}$$

where $\boldsymbol{x}(n) = [\boldsymbol{x}_1(n); \boldsymbol{x}_s(n); \boldsymbol{x}_c(n); \boldsymbol{y}(n-1); \boldsymbol{c}(n)]$ and $\boldsymbol{w} = [\boldsymbol{w}_1; \boldsymbol{w}_s; \boldsymbol{w}_c; \boldsymbol{w}_y; \boldsymbol{w}_{cross}]$. Each term of $\boldsymbol{x}(n)$ is defined as follows:

$$\boldsymbol{x}_1(n) = [x(n),\ x(n-1), \cdots, x(n-N+1)]^T, \tag{6a}$$

$$\boldsymbol{x}_s(n) = [\sin(\pi x(n)),\ \sin(\pi x(n-1)), \cdots, \sin(\pi x(n-N+1))]^T, \tag{6b}$$

$$\boldsymbol{x}_c(n) = [\cos(\pi x(n)),\ \cos(\pi x(n-1)), \cdots, \cos(\pi x(n-N+1))]^T, \tag{6c}$$

$$\boldsymbol{y}(n-1) = [y(n-1), \cdots, y(n-L)]^T, \text{ and} \tag{6d}$$

$$\boldsymbol{c}(n) = [y(n-1)\sin(\pi x(n), \cdots, y(n-1)\cos(\pi x(n-L+1)), y(n-2)\sin(\pi x(n), \cdots, y(n-L)\cos(\pi x(n-L+1))]^T. \tag{6e}$$

It should be noted that, for acquiring the reference vectors $\boldsymbol{x}(n)$, the first four vectors are easy to obtain by shifting and adding new values. In contrast, for computing the cross terms in $\boldsymbol{c}(n)$, it is difficult to update using the same approach. To reduce the complexity, only the first L terms of $\boldsymbol{x}_s(n)$ and $\boldsymbol{x}_c(n)$ are used and the matrix $\boldsymbol{c}(n)$ is decomposed into the following two matrixes:

$$\begin{bmatrix} y(n-1)\sin(\pi x(n)) & y(n-1)\sin(\pi x(n-1)) & \cdots & y(n-1)\sin(\pi x(n-L+1)) \\ y(n-2)\sin(\pi x(n)) & y(n-2)\sin(\pi x(n-1)) & \cdots & y(n-2)\sin(\pi x(n-L+1) \\ \vdots & \vdots & \vdots & \vdots \\ y(n-L)\sin(\pi x(n)) & y(n-L)\sin(\pi x(n-1)) & \cdots & y(n-L)\sin(\pi x(n-L+1) \end{bmatrix} \text{ and} \tag{7a}$$

$$\begin{bmatrix} y(n-1)\cos(\pi x(n)) & y(n-1)\cos(\pi x(n-1)) & \cdots & y(n-1)\cos(\pi x(n-L+1)) \\ y(n-2)\cos(\pi x(n)) & y(n-2)\cos(\pi x(n-1)) & \cdots & y(n-2)\cos(\pi x(n-L+1) \\ \vdots & \vdots & \vdots & \vdots \\ y(n-L)\cos(\pi x(n)) & y(n-L)\cos(\pi x(n-1)) & \cdots & y(n-L)\cos(\pi x(n-L+1) \end{bmatrix}. \tag{7b}$$

At each time *n*, the new data $\sin(\pi x(n))$, $\cos(\pi x(n))$, and $y(n-1)$ are acquired and the new reference matrixes are obtained by shifting the original elements of the matrixes by one unit from the top left corner to the bottom right corner along the main diagonal and the first rows and first columns of the new matrixes are filled with the computation results of the new data. In this way, the $\boldsymbol{c}(n)$ terms are updated with less computational effort.

As we know, the sound field inside a car is complicated and is caused by many excitation sources (Samarasinghe *et al.*, 2016). If we adopt the vibrational signals of a car's body as reference signals to control the interior noise, then multiple reference signals are required to increase the coherence between the reference signals and the noise (Sutton *et al.*, 1994, Cheer and Elliott, 2013). In this paper, we use six reference signals to reduce noise at one error microphone with one loudspeaker as an actuator. The diagram of the ANC system is displayed in Figure 4. All the controllers W_i, $\mathrm{i} = 1, \cdots, 6$, have the structure shown in Figure 3. The resultant error signal of this control system is derived as:

$$e(n) = d(n) - \hat{d}(n) = d(n) - s(n) * \sum_{i=1}^{6} y_i(n) \tag{8}$$

where $*$ denotes convolution. By taking the square of the above instantaneous error as a cost function and using the steepest descent method (Haykin, 2002), the update equation of each adaptive filter is obtained as:

$$\boldsymbol{w}_i(n+1) = \boldsymbol{w}_i(n) + \mu / [\delta + norm(\boldsymbol{x}_{if})] e(n) \boldsymbol{x}_{if}(n), \quad i = 1, 2, \cdots, 6 \tag{9}$$

where $\boldsymbol{w}_i(n)$ is the *i*th control filter $W_i(\mathrm{z})$ in the time domain and μ is a step size for updating the control filter, and $\boldsymbol{x}_{if}(n)$ is the *i*th filtered reference signal vector as $\boldsymbol{x}_{if}(n)=[\boldsymbol{x}_{i1f}(n);\boldsymbol{x}_{isf}(n);\boldsymbol{x}_{icf}(n);\boldsymbol{y}_{if}(n-1);\boldsymbol{c}_{if}(n)]$. Normalisation is applied here by dividing μ with the norm of the filtered reference vector plus a constant δ. The terms $\boldsymbol{x}_{i1f}(n)$, $\boldsymbol{x}_{isf}(n)$, $\boldsymbol{x}_{icf}(n)$, and $\boldsymbol{y}_{if}(n-1)$ at each time *n* can be readily obtained through a shift operation and adding new values. For the computation of the filtered cross terms $\boldsymbol{c}_{if}(n)$, the same method as used for updating $\boldsymbol{c}(n)$ is used.

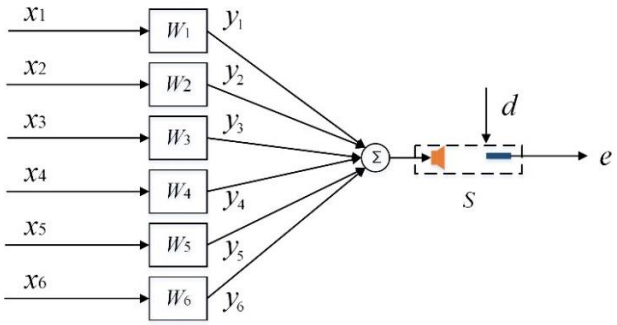

Figure 4: Diagram of the ANC system with six channels.

4 SIMULATIONS

In this section, simulations are conducted using data measured from a car driving at a third gear of 60 km/h over a coarse road with a sampling frequency of 1600 Hz. Six vibrational signals were adopted as reference signals to increase the coherence of the calculations. They were the vibrations in the *x*, *y*, and *z* directions of the front chassis; in the *y* and *z* directions of the middle chassis; and in the *x* direction of the rear chassis, where *x*, *y*, and *z* represent the front–rear, right–left, and vertical directions, respectively.

Here, the control performance of the proposed BFTLMS algorithm is compared with that of the traditional FXLMS algorithm. The parameters for the BFTLMS algorithm are $N=100$, $L=50$, $\delta=0.1$, and $u=0.0003$. For the FXLMS algorithm, the parameters for each controller are $N=128$, $\delta=0.1$, and $u=0.0002$. The simulation results in the time and frequency domains are shown in Figure 5 and Figure 6, respectively.

In Figure 5, the red line denotes the undesired noise, which is the noise before control. The green line and blue line show the resulting noises after control using the FXLMS and BFTLMS algorithms, respectively. It can be observed that, after running for 0.5 s, the controller starts to work and the noise is reduced from then on under both algorithms. Comparing the blue curve with the green curve, we also find that, in most cases, the amplitude of the blue curve is smaller than that of the green line, which means the proposed BFTLMS algorithm has better noise reduction performance.

The control results in the frequency domain are shown in Figure 6, which shows the noise level in the range 10–150 Hz without A-weighting. The noise reduction is defined as:

$$Reduction = 10\lg(d^2(\mathrm{n})/e^2(\mathrm{n})) \tag{10}$$

In Figure 6 (a), the red line denotes the undesired noise. The peaks between 25 Hz and 35 Hz are caused by the resonance of the car and the peak at 87 Hz is caused by the engine. After control, the noise corresponding to engine frequency is distinctly reduced for both algorithms and the reduction is 7dB, which can be observed from Figure 6 (b). This is because engine noise is a sinusoidal noise, which can be predicted using both linear and nonlinear controllers. For the noise between 25 Hz and 35 Hz, the BFTLMS algorithm reduces it more clearly than the linear FXLMS algorithm with the maximal reduction of 14 dB. While the linear FXLMS algorithm only achieves 6 dB reduction. Therefore, the main advantage of the BFTLMS algorithm is reducing the resonance frequencies of the car.

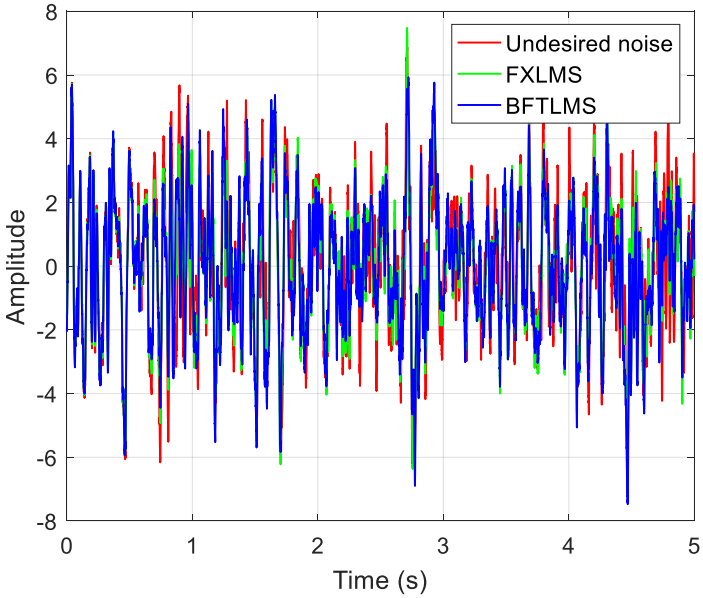

Figure 5: Control results in the time domain.

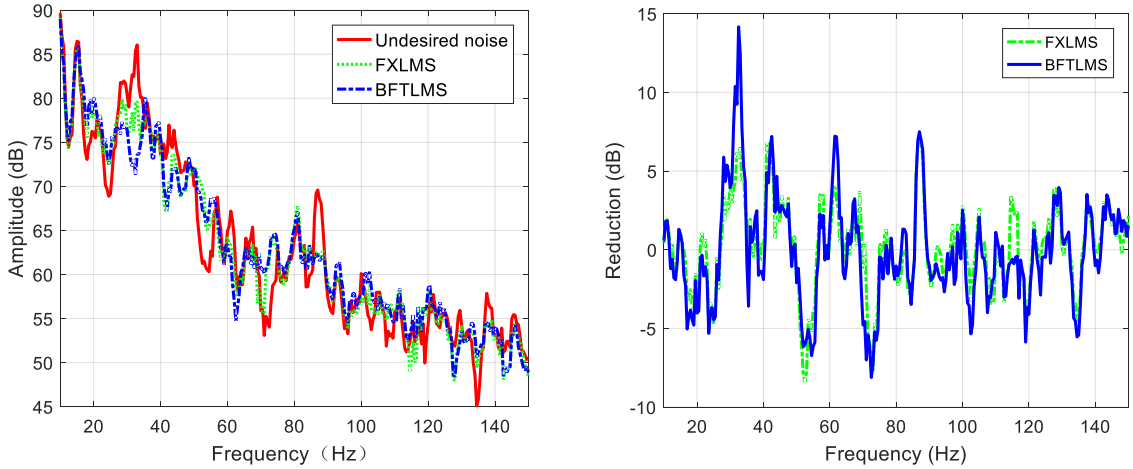

(a) (b)

Figure 6: Control results in the frequency domain: (a) amplitudes of noise before and after control and (b) noise reductions of two algorithms.

5 CONCLUSIONS

This paper analysed the specific impact and limitations of a nonminimum-phase secondary path on control performance. To improve the noise reduction performance, a nonlinear controller was proposed using a bilinear filter and trigonometric expansions. A six-channel control structure was designed to reduce road noise inside a car using six vibrational signals as reference signals. The proposed bilinear filtered trigonometric expansions least mean square (BFTLMS) algorithm was verified by simulations and the control results were compared with those of a linear filtered-x least mean square (FXLMS) algorithm in the time and frequency domains. The simulation results showed that the proposed BFTLMS algorithm outperforms the linear FXLMS algorithm, especially for reducing the noise caused by the resonance of a car.

ACKNOWLEDGEMENTS

This work was supported financially by the China Scholarship Council (CSC) and the University of Western Australia.

REFERENCES

Akhtar, MT; Abe, M; and Kawamata, M. 2006. 'A New Variable Step Size LMS Algorithm-Based Method for Improved Online Secondary Path Modeling in Active Noise Control Systems'. *IEEE Transactions on Audio, Speech, and Signal Processing* 14 (2): 720–726. doi: 10.1109/TSA.2005.855829.

Cheer, J, and Elliott SJ. 2013. 'Multichannel feedback control of interior road noise'. *The Journal of the Acoustical Society of America* 133 (5): 3588. doi: 10.1121/1.4799168.

Hansen, Colin; Snyder, Scott; Qiu, Xiaojun; Brooks, Laura; and Moreau, Danielle. 2012. *Active Control of Noise and Vibration, Second Edition*, CRC Press.

Kuo, Sen M, and Morgan, Dennis. 1995. *Active Noise Control Systems: Algorithms and DSP Implementations*: John Wiley & Sons, Inc.

Milani, Ali A; Kannan, Govind; and Panahi, Issa MS. 2010. 'On Maximum Achievable Noise Reduction in ANC Systems' 2010 IEEE International Conference on Acoustics Speech and Signal Processing (ICASSP).

Oppenheim, Alan V; Willsky, Alan S; and Nawab, S Hamid. 1996. *Signals & Systems*. Prentice-Hall, Inc.

Loiseau, Paul; Chevrel, Philippe; Yagoubi, Mohamed; and Duffal, Jean-Marc. 2015. 'Broadband Active Noise Control Design through Nonsmooth H_∞ Synthesis'. *IFAC-PapersOnLine* 48 (14): 396–401. doi: 10.1016/j.ifacol.2015.09.489.

Samarasinghe, Prasanga N; Zhang, Wen; and Abhayapala, Thushara D. 2016. 'Recent Advances in Active Noise Control Inside Automobile Cabins: Toward Quieter Cars'. *IEEE Signal Processing Magazine* 33 (6): 61–73. doi: 10.1109/msp.2016.2601942.

Haykin, Simon S. 2002. *Adaptive Filter Theory*. Vol. 2, *Prentice Hall*.

Strauch, Paul, and Mulgrew, Bernard. 1998. 'Active Control of Nonlinear Noise Processes in a Linear Duct'. *IEEE Transactions on Signal Processing* 46 (9): 2404–2412. doi: 10.1109/icassp.1997.599656.

Sutton, Trevor J; Elliott, Stephen J; McDonald, A Malcolm; and Saunders, Timothy J. 1994. 'Active Control of Road Noise Inside Vehicles'. *Noise Control Engineering Journal* 42 (4). doi: 10.3397/1.2828351.

Widrow, Bernard. 1990. *Adaptive Inverse Control*. *SPIE Proceedings* Vol. 1294: The International Society for Optics and Photonics.

Yang, Tiejun; Zhu, Liping; Li, Xinhui; and Pang, Lihong. 2018. 'An Online Secondary Path Modeling Method with Regularized Step Size and Self-tuning Power Scheduling'. *The Journal of the Acoustical Society of America* 143 (2): 1076–1084. doi: 10.1121/1.5024517.